Low-frequency relaxation processes in single-crystal proustite, Ag_3AsS_3

1989 J. Phys.: Condens. Matter 1 7669

(http://iopscience.iop.org/0953-8984/1/41/019)

J. Phys.: Condens. Matter 1 (1989) 7669–7679. Printed in the UK

Low-frequency relaxation processes in single-crystal proustite, Ag_3AsS_3

S R Yang, K N R Taylor and F Y Zhang
Advanced Electronic Materials Group, School of Physics, University of New South Wales, PO Box 1, Kensington, NSW 2033, Australia

Received 21 June 1988, in final form 9 May 1989

Abstract. Measurements of the complex dielectric constant of single-crystal proustite over the frequency range 10^{-2}–5×10^6 Hz have shown the presence of a temperature-dependent relaxation process with characteristic times of between 1×10^{-2} and 6.5×10^{-4} s. Three activation energies are observed in the resistance measurements which correlate with reported phase transitions in this material.

The dielectric relaxation can be interpreted in terms of a combined model, in which the 'Universal' dielectric dispersion law describing the anomalous low-frequency behaviour is combined with a two-layer Maxwell–Wagner model to account for the relaxation processes. The limited dielectric properties of the material have been established.

1. Introduction

High-quality, single-crystal proustite (Ag_3AsS_3) has attracted considerable attention during the past two decades because of the unusual nature of its physical properties and its potential for device applications in both non-linear optics and acousto-electronic systems [1, 2].

Among the various physical properties, the dominant interest has been in the electrical and optical properties of this material, since they relate directly to its technological importance. It has been established [3, 4] that this compound exhibits mixed electronic and ionic conduction, and that the ionic component dominates the conductivity at temperatures in excess of 230 K, with a transport number of 1.02. Dielectric dispersion studies have shown [3, 5] that proustite exhibits a very large room-temperature dielectric constant at low frequencies ($\simeq$3000 at 1 KHz) and much lower values ($\simeq$22) at frequencies greater than 1 MHz.

A detailed literature survey, carried out in the course of this work, has shown that most of the conductivity and dielectric constant measurements have been made with respect to temperature, and very little information exists with respect to the frequency dependence of the individual components of the complex dielectric constant, especially at very low frequencies. This lack of detailed knowledge is unfortunate, in view of the importance of this frequency range in applications technology. The limited publications available [3, 6] that consider the relaxation processes in this material provide an incomplete picture of its properties, and it has been concluded [3] that the frequency dependence of the conductivity and dielectric constant can not be described by a simple Debye relaxation model.

0953-8984/89/417669 + 11 $02.50

In recent years, however, it has been realised that the low-frequency response of many materials follows a similar pattern [7], particularly for those solids whose dielectric susceptibility involves a significant contribution from charge transport. Typical of this behaviour is the appearance of an anomalous low-frequency dispersion (ALFD) [8, 9] whose detailed physical origin is still not well understood.

As part of a detailed investigation of the electrical and optical properties of proustite over a wide frequency range [10–12] we have investigated the relaxation processes from 10^{-2} to 5×10^6 Hz at various temperatures between 82 K and 293 K. The results of this study show a relaxation behaviour that cannot be classified by a simple Debye model. At the frequency for which $\varepsilon'(\omega)$ shows evidence for a typical relaxation process, $\varepsilon''(\omega)$ reaches a plateau with no signs of the anticipated maximum dielectric loss. At low frequencies there is also a well established ALFD process observed at room temperature, which we believe may arise from the thermally excited Ag^+ ion charge carriers. In order to account for these observations, this work combines the 'Universal' dielectric dispersion law [7] into the well known Maxwell–Wagner two-layer model.

2. Experimental

The specimen used in this study was a synthetic single crystal cut into the form of a parallelepiped with dimensions $4.60 \times 4.30 \times 4.60$ mm^3, the edges being parallel to the x, y and z axes of the crystal respectively.

The AC conductivity, and dielectric constant measurements were carried out with the electric field parallel to the y axis (i.e. perpendicular to the crystallographic c axis). Contacts were made using silver paste electrodes and a number of AC bridges were employed during the observations. The very low-frequency (10^{-2}–10^3 Hz) measurements were made using a computer-based four-terminal impedance spectrometer with an accuracy of 0.1% [13]. The audio-frequency (200 Hz–50 kHz) and radio-frequency (50 kHz–5 MHz) measurements employed a Wayne–Kerr B224 and B601 admittance bridges with experimental precisions of better than ±0.3%.

Proustite is known to be a photosensitive semiconductor, and even very low light levels cause significant changes in the measured values of the complex dielectric constant [11, 14, 15]. Furthermore, these effects have a long recovery time after the illumination is removed, and the measured values of both the AC conductivity and dielectric constant depend upon the illumination and thermal history [1, 16, 17]. To avoid time-dependent changes originating from these effects, the specimen was maintained continuously in total darkness, and measurements were only commenced several days after sealing the cryostat.

In order to prevent the growth of silver dendrites at the electrodes, due to the high silver-ion mobility in this material, very small voltages were applied to the electrodes during the observations. For the very low-frequency measurements these were <0.1 mV peak to peak and for the others <0.5 V peak to peak. The temperature-dependence data were taken at intervals of 2–5 K and between 5 and 7 points per decade were obtained for the frequency-dependence measurements. Temperature stability was controlled to within ±1 K.

The frequency dependence of the real part of the complex dielectric constant, ε', obtained using these systems is shown in figure 1(a) for several temperatures between 82 K and 293 K. As may be seen, at the lowest frequencies the dielectric constant reaches extremely high values, being close to $\varepsilon' = 10^6$ at room temperature. As the frequency

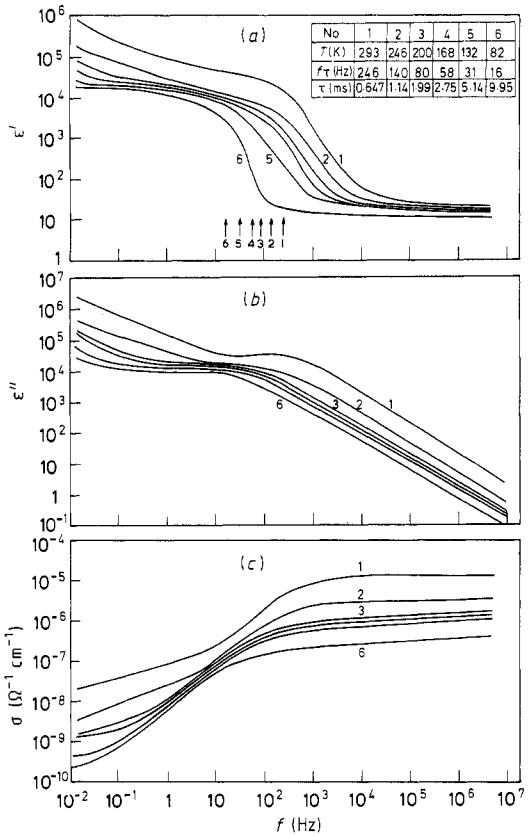

Figure 1. The frequency dependence of (*a*) the real part of the complex dielectric constant, (*b*) the imaginary part, and (*c*) the derived AC conductivity at various temperatures between 82 K and 293 K. The relaxation frequencies defined in the text are indicated for the various temperatures and the inset tabulates these frequencies along with the relaxation times.

increases, the values rapidly decrease, showing an ALFD behaviour with slope of -0.62. In the frequency range 10^2–10^4 Hz at room temperature, ε' decreases rapidly by almost three orders of magnitude to an approximate constant high-frequency value in a manner typical of a relaxation process.

The relaxation frequency in the ε' response can be defined where $\omega\tau = 1$ and $\varepsilon' = (\varepsilon'_s + \varepsilon'_\infty)/2$. These frequencies are indicated in figure 1(*a*) and the corresponding relaxation times are tabulated in the inset. At room temperature, this high-frequency value corresponds to $\varepsilon' = 22.5$ in agreement with other published values [1, 3]. Finally, it is evident from figure 1(*a*) that the relaxation frequency decreases with temperature, indicating an increase in the characteristic time for this relaxation.

The imaginary part of the dielectric constant, ε'', and the derived conductivity, σ, are shown in figure 1(*b*) and (*c*), as a function of frequency at a number of temperatures between 82 K and 293 K. In contrast to the behaviour expected for a Debye relaxation process, ε'' does not pass through a maximum at any frequency, but rather shows a continuous decrease with frequency, which is broken only by a small plateau region at a frequency slightly less than that of the ε' relaxation in figure 1(*a*). This is frequently referred to as a 'non-Debye' relaxation process.

At low frequencies, the conductivity data show a continuous increase with frequency that is frequently observed for solids in which charge carrier hopping dominates the conduction process [7]. The mechanism responsible for this behaviour was discussed originally by Pollak and Gaballe [18] for chalcogenide glasses and subsequently by Jonscher [7] who applied it to a wide range of materials. We believe that the same model

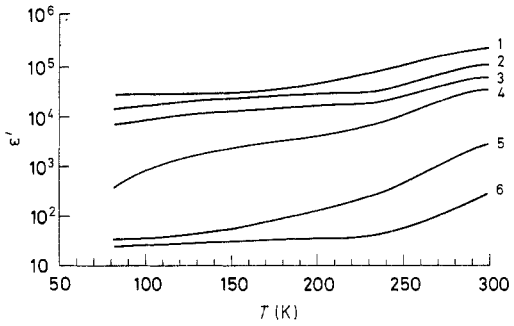

Figure 2. The temperature dependence of the real part of the complex dielectric constant at various frequencies. The curves correspond to 1 0.17 Hz, 2 1.36 Hz, 3 10.8 Hz, 4 122 Hz, 5 1 kHz and 6 10 kHz.

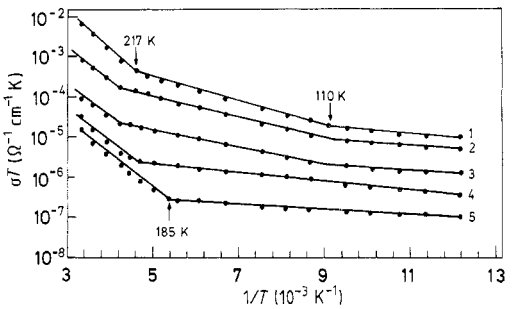

Figure 3. The variation of $\log(\sigma T)$ with $1/T$ at several frequencies, showing the three well defined linear regions at 10000, 122 and 10.8 Hz. The curves correspond to 1 10 kHz, 2 122 Hz, 3 10.8 Hz, 4 1.36 Hz and 5 0.17 Hz.

may be applied to proustite in which Ag^+ ions execute a thermally driven hopping motion through the lattice. The assumption is supported by the observation (figure 1) that the low-frequency dispersion of the dielectric constant ε' becomes stronger with increasing temperature, a behaviour that results from the increased thermal excitation of the silver ions. It is worth noting that the ionic hopping motion contributes to both components of the complex dielectric constant since it can oscillate within a normal lattice site as a dipole, and suffer scattering during its extended hopping motion [7].

The temperature dependencies of the dielectric constant and the conductivity are shown in figures 2 and 3. Figure 2 shows that the increase in ε' with temperature occurs in two ranges. Below 230 K the rise is relatively slow compared with the much faster increase beyond this temperature. It is noticeable in these data that the overall increase is faster at 122 Hz and 1 kHz than it is at other frequencies, a fact that we believe is associated with the proximity of these two frequencies to the relaxation frequency. The mechanism responsible for this will be discussed later.

As may be seen from figure 3, the $\log(\sigma T)$ versus $1/T$ variation exhibits a number of linear regions over the temperature range studied, implying the existence of a number of activation processes in the conduction mechanism. Using the usual relation for ionic conductors, i.e. $\sigma T \propto \exp(-E/kT)$, we obtain the values of the activation energy shown in table 1. It is interesting to note that the intermediate energy processes ($E \simeq 0.06$ eV) which occurs between 110 K and 220 K vanishes for frequencies less than approximately 10 Hz.

3. Discussion

It has long been known that dielectric relaxation effects can occur through a Maxwell–Wagner two-layer structure [19, 20] in which the space charge interfacial region and the

Table 1. Temperature variation of activation energy

Frequency (Hz)	10 K			122			10.8		
Region	A	B	C	A	B	C	A	B	C
Temperature range (K)	293–217	217–110	110–82	293–236	236–104	104–82	293–236	236–111	111–82
E (meV)	189	60	17	163	50.6	14.3	159	43	11.7

	Average[a]			Figure 7[b]			1 K ([24])		
Region	A	B	C	A	B	C	A′	B′	C′
Temperature range (K)				293–223	223–109	109–82	250–200	200–160	below 160
E (meV)	170	51	14.3	156	61	14.3[c]	200	60	90

[a] Average values using the data for the three frequencies above.
[b] Values taken from the fitting parameters describing the temperature dependence of the relaxation time.
[c] Average value, see text.

crystalline bulk form a layered dielectric. In such a system both layers have their own characteristic dielectric constant, conductivity and thickness as shown in figure 4(a), in conjunction with the equivalent RC circuit. The apparent dielectric properties for such a model are given by:

$$\sigma = \sigma_\infty + (\sigma_s - \sigma_\infty)/(1 + \omega^2\tau^2) \qquad \varepsilon' = \varepsilon'_\infty + (\varepsilon'_s - \varepsilon'_\infty)/(1 + \omega^2\tau^2) \tag{1}$$

where

$$\sigma_s = d/(d_1/\sigma_1 + d_2/\sigma_2)$$
$$\sigma_\infty = d(d_1\sigma_1/\varepsilon_1'^2 + d_2\sigma_2/\varepsilon_2'^2)/(d_1/\varepsilon'_1 + d_2/\varepsilon'_2)^2 \tag{2}$$

$$\varepsilon'_s = d(d_1\varepsilon'_1/\sigma_1^2 + d_2\varepsilon'_2/\sigma_2^2)/(d_1/\sigma_1 + d_2/\sigma_2)^2$$
$$\varepsilon'_\infty = d/(d_1/\varepsilon'_1 + d_2/\varepsilon'_2) \tag{3}$$

$$\tau = \varepsilon_0(\varepsilon'_1 d_2 + \varepsilon'_2 d_1)/(\sigma_1 d_2 + \sigma_2 d_1) = \varepsilon_0(\varepsilon'_s - \varepsilon'_\infty)/(\sigma_\infty - \sigma_s) \tag{4}$$

where ε_0 is the permittivity of free space.

When this two-layer model is used in connection with the frequency-dependent complex dielectric constant it is generally assumed that both the low- and high-frequency limits of ε'_s, σ_s and ε'_∞, σ_∞ are frequency-independent constants [19–21], leading to the typical two-layer relaxation spectrum shown in figure 4(b). It is clear however, from the relations shown in equations (2) and (3) that these limiting values must depend on both temperature and frequency through the material parameters ε'_1, ε'_2, σ_1, σ_2, d_1 and d_2. Consequently some considerable attention must be given to the selection of these fitting constants. As may be seen from figure 1(a) and (c), both ε' and σ tend to constant values as $\omega \to \infty$ and in this case the high-frequency limits ε'_∞ and σ_∞ can be determined unambiguously (see table 2 for values).

The assignment of the low-frequency limits ε'_s and σ_s is much more difficult, however, since both terms vary continuously as $\omega \to 0$, as many be seem from figure 1. Clearly, in order to determine these fitting parameters it is necessary to adopt some model for this low-frequency behaviour. In the present work we will adopt the proposal of Jonscher [22] which was developed by Dissado and Hill [9] in terms of the many-body interactions

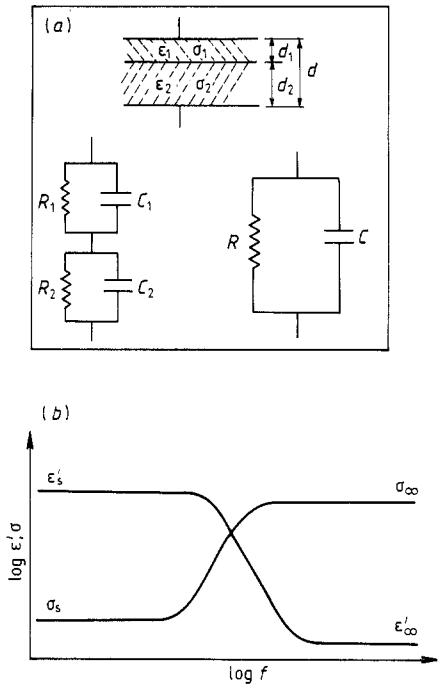

Figure 4. (*a*) The two-layer dielectric model showing the four-component circuit and the two-component equivalent circuit. $\varepsilon'_1, \varepsilon'_2, \sigma_1, \sigma_2, d_1, d_2$ are the dielectric constant, conductivity, and thickness of the space charge layer and the bulk material, respectively. (*b*) The predicted frequency dependence of both ε' and σ derived for this simple model.

between the charge carriers in the solid. In this approach the dielectric response of most materials follows a 'Universal' empirical law, namely

$$\varepsilon'(\omega) - \varepsilon'_\infty \propto \varepsilon''(\omega)\,\omega^{-p} \qquad \omega < \omega_c \tag{5}$$

and

$$\varepsilon'(\omega) - \varepsilon'_\infty \propto \varepsilon''(\omega) \propto \omega^{n-1} \qquad \omega > \omega_c$$

where ω_c is the crossover frequency of the ε' and ε'' relations, and the exponents of $p > 0$ and $n < 1$. From the relation $\sigma(\omega) = \omega\varepsilon_0\varepsilon''(\omega)$, we have

$$\sigma(\omega) \propto \omega^{1-p} \qquad \omega < \omega_c \tag{6}$$

and

$$\sigma(\omega) \propto \omega^n \qquad \omega > \omega_c.$$

In keeping with other workers adopting the two-layer model [19–21] we shall assume that the real part of the dielectric constant is unchanged between the layers (i.e. $\varepsilon'_1 = \varepsilon'_2$) and, for simplicity, we shall also assume that the parameters describing the individual bulk and space charge layers have the same frequency dependence as given

Table 2. Fitting parameters used in figure 6.

$\varepsilon'_s(f_c = 7.5\ \text{Hz}) = 3.5 \times 10^4$	$\sigma_s(f_c = 7.5\ \text{Hz}) = 2.48 \times 10^{-7}$
$\varepsilon'_\infty = 22.5$	$\sigma_\infty = 1.2 \times 10^{-5}\ (\Omega\ \text{cm})^{-1}$
$\tau = 6.47 \times 10^{-4}\ \text{s}$	$f_c = 7.5\ \text{Hz}$
$A = 3.07 \times 10^{-5}\ \text{s}^{-0.62}$	$B = 195$
$C = 4.8 \times 10^{-8}\ (\Omega\ \text{cm})\ \text{s}^{-0.38}$	$p = 0.62$

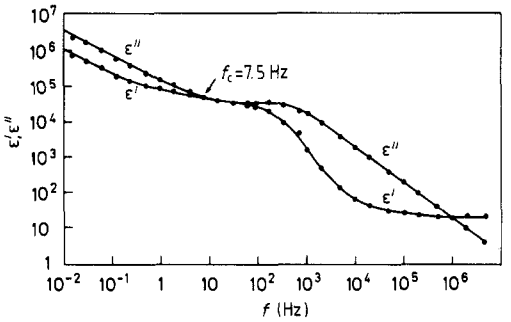

Figure 5. The experimental room-temperature variation of both ε' and ε'' with frequency, showing a crossover frequency of $f_c = 7.5$ Hz.

by equations (5) and (6), and under these conditions we have then

$$\begin{aligned}
&\varepsilon_1'(\omega) = \varepsilon_2'(\omega) = \xi_0\omega^{-p} + \varepsilon_\infty' && \omega < \omega_c \\
&\varepsilon_1'(\omega) = \varepsilon_2'(\omega) = \xi_0\omega^{n-1} + \varepsilon_\infty' && \omega > \omega_c \\
&\left.\begin{aligned}\sigma_i(\omega) &= \sigma_{i0}\omega^{1-p}\\ \sigma_i(\omega) &= \sigma_{i0}\omega^{n}\end{aligned}\right\}\text{for } i = 1, 2 && \begin{aligned}&\omega < \omega_c\\ &\omega > \omega_c\end{aligned}
\end{aligned} \tag{7}$$

where ξ_0, σ_{i0} are constants.

Since the space charge layer thickness d_1, is a slowly varying function of frequency [23], it maybe assumed to be constant over the relatively small frequency range $\omega\tau \ll 1$ involved here.

In order to evaluate the limiting values ε_s' and σ_s (for $\omega\tau \ll 1$) we can substitute the expressions of equation (7) into equations (2) and (3) to give

$$\left.\begin{aligned}\varepsilon_s' &= A\omega^{-p} + B\\ \sigma_s &= C\omega^{1-p}\end{aligned}\right\} \qquad \text{for } \omega < \omega_c \tag{8}$$

and derive the constants A, B, C and p by fitting to the experimental data. In these expressions, the coefficients are independent of frequency within the assumptions being made, and are given by:

$$\begin{aligned}
A &= d(d_1/\sigma_{10}^2 + d_2/\sigma_{20}^2)\xi_0/(d_1/\sigma_{10} + d_2/\sigma_{20})^2\\
B &= d(d_1/\sigma_{10}^2 + d_2/\sigma_{20}^2)\varepsilon_\infty'/(d_1/\sigma_{10} + d_2/\sigma_{20})\\
C &= d/(d_1/\sigma_{10} + d_2\sigma_{20}).
\end{aligned} \tag{9}$$

These constants involved in this fitting procedure for the low-frequency data are given in table 2.

In order to obtain the best fit of $\log \varepsilon'$ versus $\log \omega$ and $\log \sigma$ versus $\log \omega$ variations we can substitute the limiting values ε_s' and σ_s from equation (8) into equation (1). Following other workers we will assume that in doing so then ε_s' and σ_s for frequencies $\omega > \omega_c$ may be treated as constants given by

$$\left.\begin{aligned}\varepsilon_s' &= \varepsilon_s'(\omega = \omega_c)\\ \sigma_s &= \sigma_s(\omega = \omega_c)\end{aligned}\right\} \qquad \text{for } \omega > \omega_c. \tag{10}$$

This approach has been generally adopted [19–21] and shown to hold. The crossover frequency used in the present work has been taken to be $f = 7.5$ Hz as indicated by figure 5, which shows the full experimental frequency dependence of both ε' and ε'' at room

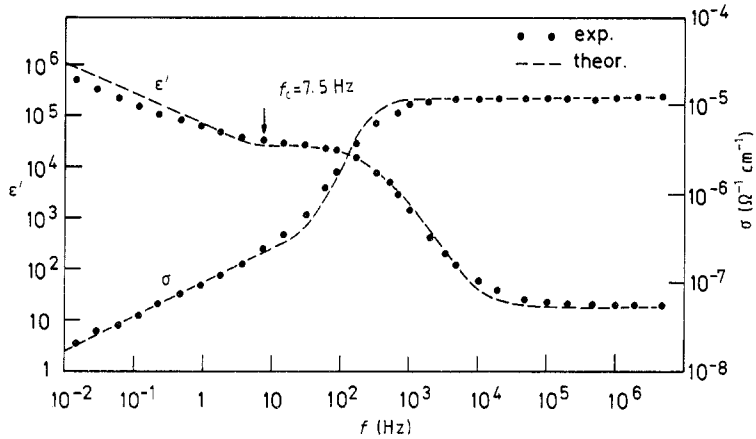

Figure 6. Comparison of the experimental data ($T = 293$ K, full circles) with the theoretical predictions (broken curves) for both log ε' versus log f and log σ versus log f. The parameters corresponding to the theoretical fit are given in Table 2.

temperature. For low-frequency limits of ε'_s and σ_s for $\omega > \omega_c$ thus determined, see table 2.

The predicted frequency dependences of both ε' and σ at room temperature obtained in this way and using the constants of table 2 are shown in figure 6 along with the experimental data for comparison.

The close agreement between the theoretical and experimental data points give strong support to the use of a combined model of the dielectric response at low frequencies in materials with inhomogenous, carrier dominated conductivity. The relatively small discrepancies observed in figure 6 may be associated with the assumptions concerning the dielectric constant in the two layers and that the thickness terms are frequency independent.

We are now in a position to discuss the temperature dependence of the dielectric response shown in figures 2 and 3. The rapid increase of ε' above 230 K (figure 2) is obviously due to the increasing contribution from the thermally excited Ag^+ ion hopping motion as mentioned above. The relatively faster change in ε' with temperature observed in the intermediate frequency range (100–1000 Hz) may be understood in terms of the Maxwell–Wagner model. At high frequencies, say $f = 10$ kHz, $\omega\tau \gg 1$ and $\varepsilon' \to \varepsilon'_\infty$, consequently

$$\mathrm{d}\varepsilon'(\omega)/dT \simeq \mathrm{d}\varepsilon'_\infty/\mathrm{d}T \qquad \omega\tau \gg 1 \tag{11}$$

while at low frequencies $\omega\tau \ll 1$ and $\varepsilon' \to \varepsilon'_s$, giving

$$\mathrm{d}\varepsilon'(\omega)/\mathrm{d}T \simeq \mathrm{d}\varepsilon'_s/\mathrm{d}T \qquad \omega\tau \ll 1. \tag{12}$$

In the intermediate frequency range, however, for which $\omega\tau \simeq 1$, then

$$\mathrm{d}\varepsilon'(\omega)/\mathrm{d}T \simeq \tfrac{1}{2}\mathrm{d}/\mathrm{d}T(\varepsilon'_s + \varepsilon'_\infty) - \tfrac{1}{2}\omega(\varepsilon'_s - \varepsilon'_\infty)\mathrm{d}\tau/\mathrm{d}T. \tag{13}$$

Using these relations, it is readily shown that the temperature dependence of ε' in the intermediate frequencies, close to $\omega\tau \simeq 1$, will be significantly greater than that at other frequencies. The nature of these results is given in table 3 for a temperature of 175 K along with the experimental values.

Turning now to the temperature dependence of the relaxation mechanism as described by the time constant τ, if we assumne that the space-charge layer resistance is

Table 3. Comparison of the temperature coefficients $1/\varepsilon'(\omega)\,\mathrm{d}\varepsilon'(\omega)/\mathrm{d}T$ at 175 K. Three predicted low-frequency values were calculated using equation (11); the high-frequency 10 kHz value from equation (12), two intermediate-frequency values from equation (13) and all experimental values from figure 2. The values of $\mathrm{d}\varepsilon'_s/\mathrm{d}T = 36\,\mathrm{K}^{-1}$, $\mathrm{d}\varepsilon'_\infty/\mathrm{d}T = 4.6 \times 10^{-2}\,\mathrm{K}^{-1}$, $\mathrm{d}\tau/\mathrm{d}T = 2.4 \times 10^{-5}$ were found from figure 1(*a*).

Frequency (Hz)	$\omega\tau$	Experimental values (K^{-1})	Predicted values (K^{-1})
0.17	4.0×10^{-4}	8.1×10^{-3}	1.2×10^{-3}
0.36	3.2×10^{-3}	9.1×10^{-3}	1.5×10^{-3}
10.8	2.6×10^{-2}	6.9×10^{-3}	2.7×10^{-3}
122	2.9×10^{-1}	1.1×10^{-2}	6.4×10^{-3}
1000	2.4	1.6×10^{-2}	1.1×10^{-1}
10000	24	8.0×10^{-3}	2×10^{-3}

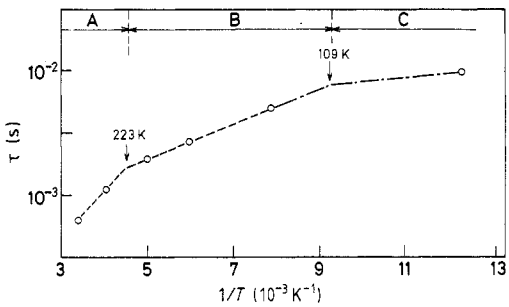

Figure 7. The variation of the relaxation times with temperature. The broken curves are fitted to the experimental data while the low-temperature (region C) curve (chain) is drawn using the average values from figure 3 and table 1 at these temperatures.

much larger than that of the bulk (i.e. $d_1/\sigma_1 \gg d_2/\sigma_2$) and that the dielectric constants of the two layers are equal (i.e. $\varepsilon'_1 = \varepsilon'_2 = \varepsilon'_\infty$) [18–21] then equation (4) reduces to

$$\tau \simeq \varepsilon_0 \varepsilon'_\infty d/d_1 \sigma_2. \tag{14}$$

Changes in τ with temperature will clearly be dominated by the behaviour of the conductivity term σ_2 ($= nq\mu$), and hence by the temperature dependence of the ionic carrier density n and the ionic mobility μ.

The carrier density and mobility can be expressed as

$$n = n_0 \exp(-\varphi/2kT) \qquad \mu = \mu_0 \exp(-U/kT) \tag{15}$$

where φ and U are the Ag^+ ion formation energy and migration energy respectively. Substituting equation (15) with the expression $\sigma = nq\mu$ into equation (14), we have for the relaxation time

$$\tau = \tau_0/d_1 \exp(E/kT) \tag{16}$$

where $E = \frac{1}{2}\varphi + U$ and $\tau_0 = \varepsilon_0 \varepsilon'_\infty d/n_0 q \mu_0$.

The experimental values of τ given in the inset to figure 1 are presented in figure 7 as a log τ versus $1/T$ variation. As may be seen, the observed data show a continuing decrease in gradient with decreasing temperature. Using equation (16) this suggests that the activation energy E is also temperature dependent in agreement with the results of figure 3. Bearing in mind that it is the conductivity in both cases that leads to the observed behaviour, we can compare the values derived from figure 3 with those obtained from the observed variation of the relaxation time shown in figure 7. At both the high (region A, 223 K $< T <$ 293 K) and intermediate (region B, 109 K $< T <$ 223 K) temperatures

of this figure this is straightforward and gives the values of $E_A = 156$ meV and $E_B = 61$ meV, which agree remarkably well with those obtained by averaging the conductivity results over the frequency range involved. These values are given in table 1 for comparison of the two sets of data. In the lowest temperature range (region C) there are insufficient data to allow any form of curve fitting and in this region we have used the average of the low-temperature values from figure 3 and table 1 as $E_c = 14.3$ meV. The theoretical variations based on these values are shown in figure 7 from which it is clear that this series of exponential terms adequately describes the data, and that both the conductivity and relaxation parameters may be described by the same process over the different temperature ranges. Other evidence for temperature-dependent activation energies had come from the work of Gorin *et al* [24], and their values, in essentially the same temperature ranges, are also given in table 1. The values in both the high and intermediate ranges are very similar to our own, but their low-temperature activation energy is almost an order of magnitude greater than ours.

Since both the present study, and the earlier work [24] identify distinct thermal processes in three ranges of temperature, it is interesting to speculate on the origin of the changes that occur between the different temperature regimes. From the data presented in figures 3 and 7 and table 1, two transition temperatures can be identified; these lie in the range $104\ \text{K} < T_1 < 111\ \text{K}$ and $185\ \text{K} < T_2 < 236\ \text{K}$. Temperatures close to these, of course, are not unknown in connection with proustite. Semak *et al* [25] associated changes in the pyroelectric behaviour at 110 K with a symmetry-lowering phase change, and optical scattering studies [26, 27] have been used to identify a second-order phase change at 210 K. These temperatures are clearly related to T_1 and T_2 derived above and suggest that we are seeing changes in the dielectric behaviour at these reported phase changes. It must be pointed out, however, that these transitions are not observed in all properties, nor in all samples, and there is considerable disagreement concerning the behaviour of proustite in these temperature ranges (see [28] and references therein). Rather than invoke a phase change at T_2 it is possible that we are seeing the changeover from electronic to ionic conductivity at this temperature that has been reported by other workers [3, 4], in which case the highest temperature activation energy (region A) relates to the motion of the Ag^+ ions throughout the lattice.

4. Conclusions

Measurements of the temperature dependence of the complex dielectric constant between 82 K and 293 K over a wide range of frequencies extending from 10^{-2} to 5×10^6 Hz have revealed the presence of a well defined relaxation process. The frequency and relaxation time of this phenomenon varies with temperature, the relaxation occurring at frequencies that decrease as the temperature decreases.

Both the observed temperature dependence of the conductivity and the derived values of the relaxation time are consistent with a mechanism involving thermally moderated activation and migration of carrier. This may be described in terms of an energy $E\ (= \varphi/2 + U)$, where φ and U are the energies involved in the formation and migration of the carriers.

Three distinct temperature regions are observed, which may be defined by the energy values $E_A = 170$ meV, $E_B = 51$ meV and $E_C = 14.3$ meV with A, B and C occurring in decreasing temperature order. The transition temperatures between these regions lie close to 110 K and 220 K respectively, and may be associated with effects at these

temperatures observed by other workers and identified as phase changes. It is possible, however, that the transition at $T \simeq 220$ K may be associated with the changeover from electronic to ionic conductivity, in which case only the upper temperature region will be associated with mobile Ag^+ ions.

The 'Universal' dielectric dispersion power law has been combined with the Maxwell–Wagner two-layer model to interpret the observed relaxation phenomena. This method has been proved to be successful by the fair agreement between the theory and experimental results.

References

[1] Bardsley W, Davies P H, Hobden M V, Hulme K F, Jones O, Pomeroy W and Warner J 1968 *Opto-electronics* **1** 29
[2] O'Hara C, Shorrocks N M, Whatmore R W and Jones O 1982 *J. Phys. D: Appl. Phys.* **15** 1289
[3] Davies P H, Elliott C T and Hulme K F 1969 *J. Phys. D: Appl. Phys.* **3** 165
[4] Zlokazov V B, Kovelev L Ya and Karpachev S V 1981 *Sov. Phys.–Dokl.* **26** 684
[5] Byer H H and Bobb L C 1974 *J. Appl. Phys.* **45** 3738
[6] Alekseeva Z M, Skorun A D and Tsivileva I M 1984 *Bull. Acad. Sci. USSR Phys. Ser.* **48** 83
[7] Jonscher A K 1983 *Dielectric Relaxation in Solids* (London: Chelsea Dielectric)
[8] Jonscher A K 1978 *Phil. Mag.* B **38** 587
[9] Dissado L A and Hill R M 1984 *J. Chem. Soc. Faraday Trans.* II **80** 291
[10] Yang S R and Taylor K N R 1986 *Sov. Phys.–Solid State* **29** 1459
[11] Taylor K N R and Yang S R 1988 *J. Appl. Phys.* **64** 2621
[12] Yang S R, Taylor K N R and Zhang F Y 1989 *J. Phys.: Condens. Matter.* **1** 1663
[13] Bell D J, Coster H G L and Smith J R 1975 *J. Phys. E: Sci. Instrum* **8** 66
[14] Gavrilova N D, Popova T V and Novik V K 1979 *Sov. Phys.–Solid State* **21** 1244
[15] Gavrilova N D, Novik V K and Popova T V 1982 *Sov. Phys.–Solid State* **24** 1735
[16] Alekseeva Z M, Skorbun A D and Tsivileva I M 1981 *Sov. J. Low Temp. Phys.* **7** 248
[17] Butsko N I, Moroz E G and Osypishin I S 1967 *J. Ukr. Phys.* **12** 1953
[18] Pollak M and Geballe T H 1961 *Phys. Rev.* **122** 1745
[19] Von Hippel A R 1959 *Dielectrics and Waves* (New York: Wiley) p 228
[20] Volger J 1960 *Progress in Semiconductors* vol 4, ed. A F Gibson (New York: Wiley) p 206
[21] Haberey F and Wigi H P J 1968 *Phys. Status Solidi* **26** 231
[22] Jonscher A K 1981 *J. Matter. Sci.* **16** 2037
[23] Chang H C and Jaffe G 1952 *J. Chem. Phys.* **20** 1071
[24] Gorin Y F, Koberlev L Ya, Babushkin A N and Zlokazov V B 1983
[25] Semak D G, Mikhalto I P, Popik Y V, Bercha D M, Nebola I I, Golovel M I and Gurzan M I 1975 *Sov. Phys–Semicond* **8** 823
[26] Smolenskii G A, Sinii I G, Kuzminov E G and Godovikov A G 1979 *Sov. Phys.–Solid State* **21** 1343
[27] Smolenskii G A, Sinii I G, Prokhorova S D, Kuzminov E G and Godovikov A G 1982 *Sov. Phys.–Crystallogr.* **27** 82
[28] Belyaev A D, Gololobov Y U, Machulin V F, Miselyuk E G and Nekrasova I M 1984 *Sov. Phys.–Solid State* **26** 820